

## **Multilayered Carbon nanotubes/polydopamine-based electrodes for hydrogen fuel cells: effect of polydopamine coverage rates on power densities**

Hongtao Long<sup>1</sup>, Doriane Del Frari<sup>1</sup>, Vincent Rogé<sup>1</sup>, Joffrey Didierjean<sup>1</sup>, Marc Michel<sup>1\*</sup>

<sup>1</sup>Luxembourg Institute of Science and Technology (LIST), Materials and Research Technology (MRT), 5 Avenue des Hauts-Fourneaux, L-4362 Esch/Alzette, Luxembourg

Corresponding Author: Hongtao Long

---

**ABSTRACT:** Polydopamine (PDA) is now considered as an interesting polymer for the design of efficient proton exchange membrane fuel cell (PEMFC) electrodes, which paves the way for high performance and stable PEMFC electrodes to be produced. This work aims at showing the effect of different surface coverage of PDA on Multi-Walled Carbon Nanotubes (MWNTs) which were used as catalytic support. The single cell test shows that the power density of the electrodes decreases when the surface covering of PDA is increased. Power densities of 350 and 600 mW.cm<sup>-2</sup> were obtained according to different surface covering of PDA. This article highlights the fact that the PDA plays an important role in electrodes allowing fuel cell efficiency to be significantly improved compared to commercial black carbon (Pt / CB) without PDA (used as a standard reference).

**Keywords:** Proton Exchange Membrane Fuel Cells (PEMFC), Membrane Electrode Assembly (MEA), Polydopamine (PDA), Power density.

---

Date of Submission: 28-02-2020

Date of acceptance: 07-03-2020

---

### **I. INTRODUCTION**

Over the past decade, Proton Exchange Membrane Fuel Cells (PEMFCs) have gained significant attention as promising power sources for transportation, portable and stationary applications as they provide a wide range of benefits, including reduced greenhouse gas emissions and increased use of renewable energy [1-3]. Nevertheless, the development of high-performance, low cost and durable catalysts is considered as an important issue to the commercialization of PEMFCs [4]. The high cost is related to the amount of Platinum, which is by now considered as one of the best catalysts for hydrogen oxidation reaction (HOR) and oxygen reduction reaction (ORR). Nevertheless, only a small percentage of Pt is accessible for the electrode layer [5] in conventional Membrane Electrode Assemblies (MEAs).

Up to now, a large number of novel catalyst systems with reduced Pt content have been developed such as: 1) the utilization of a proton conducting media such as Nafion<sup>®</sup> which is able to lower the Pt loading in electrodes [6], 2) Pt alloys and core-shell Pt nanoparticles [7,8], and 3) platinum-free electrocatalysts [9]. Additionally, one of PEMFC's most challenging cost reduction problems is to improve Pt efficiency by optimizing the Triple-Phase Boundary (TPB) where electrolytes, reactants, and electrical compounds need to be well interconnected. It is well established that the control of the TPB, is responsible for the performance in terms of power densities [10]. Hence, a strong focus of the current research is on finding the best balance between ionic and electronic conductive mediums in the MEAs, thanks to the optimization of interfaces at the nanoscale level. Up to now, the enhancement of the Platinum utilization was mainly based on the control of electrode processing technologies like sputtering methods [11] where researchers reached a Platinum utilization of 826 mW.mg<sub>(Pt)</sub><sup>-1</sup>. Tayloret al. employed nanoimprint deposition techniques [12] to prepare PEMFCs catalyst layer directly at the surface of a Nafion<sup>®</sup> membrane and Pt utilization of 15375 mW.mg<sub>(Pt)</sub><sup>-1</sup> was obtained with a low Pt loading of 0.020 mg<sub>(Pt)</sub>.cm<sup>-2</sup>.

Recently, we employed the so called "layer-by-layer" (LBL) approach [13,14], invented by Decher et al. [15], for integrating disparate materials into multi-layered thin films used as electrodes for PEMFCs. It is obtained by dipping and/or spraying [14,16,17] processes. For example, electrodes made of conductive polymers such as polyaniline have shown promising results in terms of power densities and Pt utilization with values as high as 63 mW.cm<sup>-2</sup> and 437.5 mW.mg<sup>-1</sup> respectively [18].

Another point to be considered concerns the degradation of carbon catalyst support, which is known as the primary deactivating factor of PEMFCs [19,20]. In general carbon support corrodes when high potentials

---

(0.6-1.2 V), high humidification, high temperatures (50–90°C), and high oxygen concentration [21,22] are applied. In addition, the interaction between the catalyst and the carbon support tends to aggravate this degradation. Indeed, the catalyst promotes carbon degradation because of their catalytic effect. [23]. Therefore, the electrochemical active surface area decreases, the 3D structure of electrode is damaged leading to ultimately decrease the performance of the electrode. Consequently, it is extremely crucial to search for materials able to protect carbon based electrodes against corrosion.

Very recently, we have demonstrated [19] that multi-layered anodes made of sprayed Pt/MWNTs covered with only 20% of PDA can deliver very high values of power density at  $780 \text{ mW}\cdot\text{cm}^{-2}$  while being tolerant towards corrosion. Moreover, we have shown that the concentration loss at high current density might be due to the inability of the MEA to maintain the diffusion of reagents to the catalytic site. Then we expect that we might be able to further delay the crash of this area by covering more PDA on MWNTs thanks to its unique properties [24].

This work aims at further exploring the influence of different PDA surface coverages onto carbon nanotubes on PEMFCs performances. To this aim, three electrodes made of Pt/MWNTs covered with different percentages of PDA were studied and investigated by transmission and scanning electron microscopies (TEM, SEM) for the structure, and X-ray Photoelectron Spectroscopy (XPS) in order to get access to the surface coverage of PDA coated on the surface of carbon nanotubes. Electrochemical and Polarization tests were also done to check the performance of the multi-layered electrodes with of different surface coverage of PDA.

## II. EXPERIMENTAL

In this work, the following materials were used: chloroplatinic acid hexahydrate ( $\text{H}_2\text{PtCl}_6\cdot 6\text{H}_2\text{O}$ ), dopamine hydrochloride, MWNTs (755125-1 G), and Nafion solution (5% Nafion® 1100 in a mixture of lower aliphatic alcohol and water). They were all bought out from Sigma-Aldrich.

### 2.1 Functionalization of multi-walled carbon nanotubes with Pt nanoparticles

400 mg of MWNTs were first sonicated in 50 vol%  $\text{HNO}_3$  and deionized water for 15 min, then collected in 40 ml of ethylene glycol (EG) by filtration and rinsed with deionized water. Then mixed with 400 mg of Chloroplatinic acid hexahydrate ( $\text{H}_2\text{PtCl}_6\cdot 6\text{H}_2\text{O}$ ) in 120 ml of ethylene glycol. The solution was heated to  $145^\circ\text{C}$  for 1 h under stirring. Finally, Pt/MWNTs were collected after filtration.

### 2.2 Functionalization of Pt/MWNTs with different percentages of polydopamine

400 mg Pt/MWNTs were functionalized with different amount of polydopamine precursor. To this aim, 3 samples were prepared:

$S_1$  corresponding to Pt/MWNTs made with  $0.2 \text{ mg}\cdot\text{ml}^{-1}$  of dopamine;

$S_2$  corresponding to Pt/MWNTs made with  $0.5 \text{ mg}\cdot\text{ml}^{-1}$  of dopamine;

$S_3$  corresponding to Pt/MWNTs made with  $0.8 \text{ mg}\cdot\text{ml}^{-1}$  of dopamine in 10 mM Tris-HCl (pH 8.5) (400 mL), respectively, and the solution was stirred for 24 h at room temperature by using air as oxidant. The Pt/MWNTs-(PDA) were filtered and rinsed with deionized water.

### 2.3 Preparation of MEA based on sprayed casting

The Nafion® 117 membrane was used as LBL substrate. In order to clean and protonate them a pre-treated in boiling in a 50 vol%  $\text{HNO}_3$  solution for 1 h was performed. Then they were successively rinsed in boiling deionized water for 1 h, boiling 0.5 M  $\text{H}_2\text{SO}_4$  solution for 30 min, and boiling water for 30 min. The last step in deionized water was repeated twice.

Pt/MWNTs-(PDA) were dispersed in isopropanol ( $10 \text{ mg}\cdot\text{mL}^{-1}$ ) under sonication for 15 min, 200 ml of the dispersion was sprayed onto both sides of the membrane. We accelerated the manufacturing time thanks to a heat treatment.

## 2.4 Physical characterizations

### 2.4.1 TEM analysis

The TEM analyses were applied on a ZEISS LEO922 operating at 200 kV acceleration voltage. TEM pictures were acquired in the Bright-Field (BF) mode and were registered on a TRS CCD camera.

### 2.4.2 SEM analysis

Scanning electron microscopy (SEM) with a Quanta FEG 200 (FEI Nova, Netherland) field-emission gun and operating at 15 kV was applied to investigate the morphology of the surface of MEA.

### 2.4.3 XPS analysis

X-ray photoelectron spectroscopy (XPS) characterisations were performed with a Kratos Axis ultra DLD instrument equipped with a hemispherical energy analyser and a monochromatic Al  $K_\alpha$  X-ray beam ( $E = 1486.6 \text{ eV}$ ) operated at 150 W. The pass energy (PE) was fixed at 160 eV for survey scans and 20 eV for core level

spectra. The analysis area was  $300 \times 700 \mu\text{m}^2$ . The different samples elemental composition was determined by XPS.

#### 2.4.4 TGA analysis

The thermogravimetric analysis (TGA; Netzsch STA 409 PC/PG) with a flow rate at  $80 \text{ ml} \cdot \text{min}^{-1}$  of  $\text{N}_2/\text{O}_2$  was used to quantify the Platinum loading. Samples were heated to  $1000^\circ\text{C}$  with a heating speed rate of  $20 \text{ K} \cdot \text{min}^{-1}$ .

#### 2.4.5 Electrical characterisation

Electrical conductivities were measured by a technique called four point probes (Ecopia HMS-3000 Hall Measurement System), which investigate the ohmic integrity of the samples.

#### 2.4.6 Electrochemical characterisation

Cyclic voltamograms (CVs) were performed with a Gamry Reference 600TM potentiostat (Gamry Instruments) using a glassy carbon working electrode ( $\text{Ø} = 3 \text{ mm}$ ), a Pt wire as counter electrode, and a saturated calomel electrode (ECS) as reference electrode in  $0.5 \text{ M H}_2\text{SO}_4$  (ACS reagent 70 %). The potential between the working electrode (WE) and reference electrode was cycled between  $-0.2$  to  $1 \text{ V}$  with a sweep rate of  $50 \text{ mV} \cdot \text{s}^{-1}$ . Data were collected after 200 cycles, to assure a system stability.

#### 2.5.7 Single-cell tests

The polarization curve of the MEAs were measured automatically by fuel cell test bench (FuelCon AG, Germany). MEA were firstly placed between two gas diffusion layers (GDL: H2315-13 carbon paper). The anode was fed with a flow rate of  $150 \text{ mL} \cdot \text{min}^{-1} \text{ H}_2$  with water in a humidifier ( $T=80^\circ\text{C}$ ), meanwhile, the cathode was fed with  $75 \text{ mL} \cdot \text{min}^{-1}$  of high-purity  $\text{O}_2$  with water in a humidifier at atmospheric pressure. The cell temperature was set to  $70^\circ\text{C}$ .

### III. RESULTS AND DISCUSSION

In order to investigate which role does the PDA play for MEAs, the three samples S1, S2 and S3 were prepared.

Three solutions with different concentrations of PDA precursor ( $0.2$ ,  $0.5$  and  $0.8 \text{ mg} \cdot \text{mL}^{-1}$  for A, B and C, respectively) have been used to grow PDA films with different thicknesses. As we mentioned in our previous work [19] "the presence of PDA is characterized by a uniform contrast on carbon nanotubes compared to uncovered ones", allowing us to visualise the PDA film formed around MWNTs.

Fig. 1 show transmission electron microscopy (TEM) images of Pt functionalised MWNTs covered with PDA. This figure highlights a random distribution of Pt nanoparticles on MWNTs before the deposition of PDA with S1, S2 and S3. For all three samples, the synthesized Pt nanoparticles are homogeneous in size, with diameters around  $5\text{-}10 \text{ nm}$ . Concerning the growth of PDA films around MWNTs, based on figures 1A and 1B, it is difficult to assess a full coverage of PDA using solutions S1 and S2. However, for the most concentrated solution S3, it seems that a continuous conformal layer of  $8 \text{ nm}$  has been grown around MWNTs.

It is interesting to note that for this conformal PDA layer (S3, Fig. 1C), almost all the Pt nanoparticles look strapped inside the PDA film. This may be attributed to a property of PDA to modify a variety of material's surface [24]. Unfortunately, it might also jeopardize the balance between the electronic and the ionic conductivity.

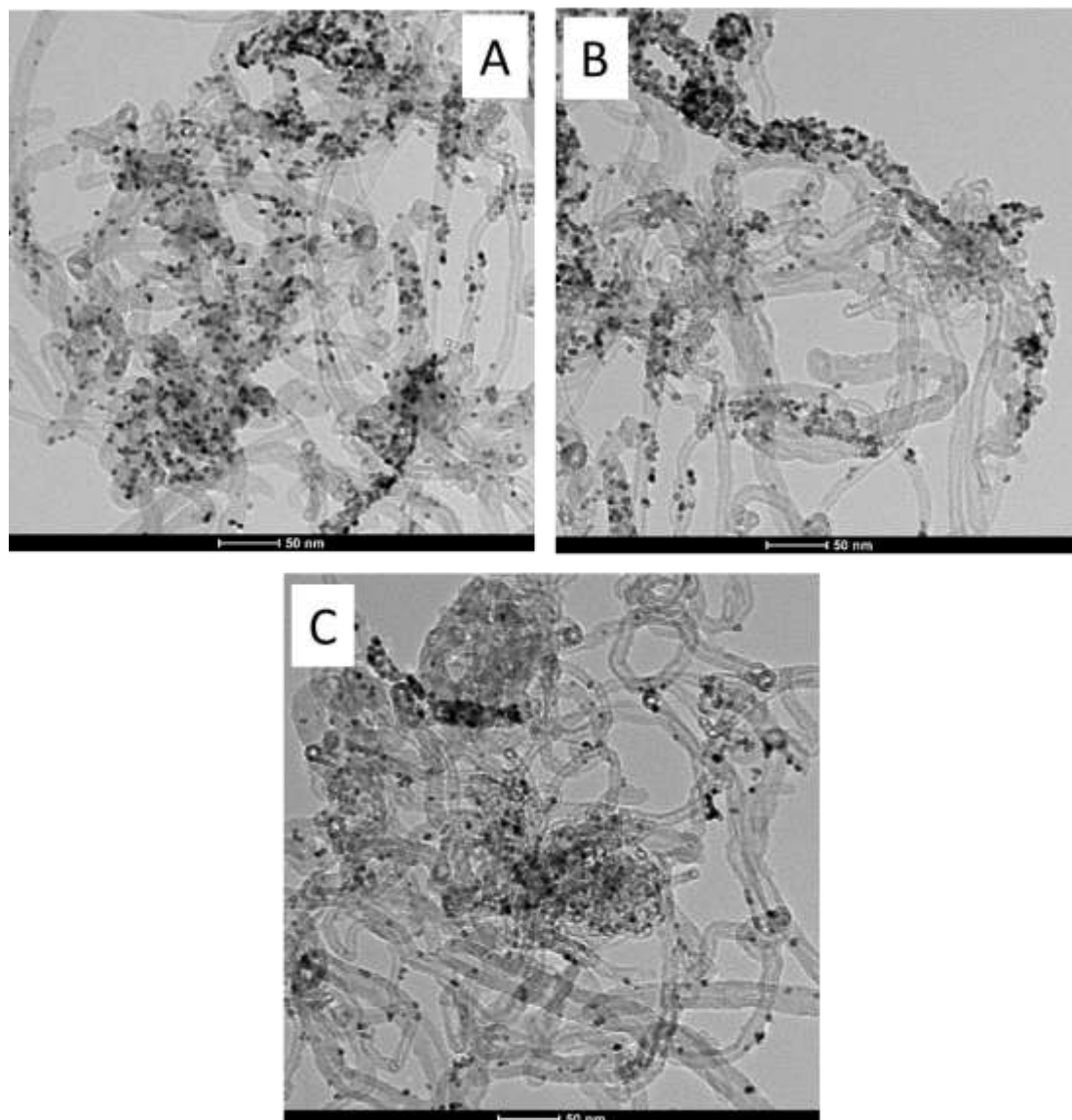


**Fig. 1.** TEM images of catalyst layer Pt/MWNTs-PDA made with different concentrations of dopamine hydrochloride: 0.2 mg.ml<sup>-1</sup>(A, corresponding to S<sub>1</sub>), 0.5 mg.ml<sup>-1</sup> (B, corresponding to S<sub>2</sub>), and 0.8 mg.ml<sup>-1</sup> (C, corresponding to S<sub>3</sub>), respectively

In order to determine if PDA forms a continuous layer even at low concentration solution, XPS measurement have been carried out. It shows (Table 1)that the nitrogen (due to the presence of PDA) is detected on all these three samples.Their N/C ratio are 3.6%, 6.1% and 6.8%, respectively. The S<sub>2</sub> with 6.1% N/C ratio is extremely close to the reference (PDA reference sample (6.8%) [19]), which means the MWNTs seems close to be fully covered with PDA. If we assume that the thickness of PDA is greater than the analytical depth of XPS (approx. between 5 and 10 nm) and that carbon-based contamination is negligible, then PDA surface coverage can be measured using the method we have developed:

$$C_{\text{PDA}} (\sigma) + C_{\text{MWNTs}} (1 - \sigma) = C_{\text{TOT}} \quad (1) \text{ where the covering}$$

$$\text{of PDA } (\sigma) \text{ can be calculated: } \sigma = \frac{N/C(\text{Sample})}{0.068} (2)$$

Therefore, according this model, the surface coverage of PDA for these samples are estimated to be 51.2%, 88.2%, and 100%, for S<sub>1</sub>, S<sub>2</sub> and S<sub>3</sub> respectively.

| Sample         | O (at%) | C (at%) | N (at%) | Ca (at%) | Pt (at%) | N/C(%) |
|----------------|---------|---------|---------|----------|----------|--------|
| S <sub>1</sub> | 10.2    | 85.0    | 3.1     | 0.3      | 1.4      | 3.6    |
| S <sub>2</sub> | 14.6    | 79.2    | 4.8     | 0.5      | 0.9      | 6.1    |
| S <sub>3</sub> | 16.0    | 77.8    | 5.3     | 0.9      | 0.0      | 6.8    |

Table1: Elemental composition of Pt/MWNTs-PDA samples (measured by XPS) made with different concentrations of dopaminehydrochloride: 0.2 mg.ml<sup>-1</sup> (S<sub>1</sub>), 0.5 mg.ml<sup>-1</sup> (S<sub>2</sub>), and 0.8 mg.ml<sup>-1</sup> (S<sub>3</sub>), respectively. The last column corresponds to N/C ratio.

The 100% estimated coverage of S<sub>3</sub> is in agreement with the continuous film observed on TEM images on Fig. 1C. Here, we confirm that the PDA covers the Pt/MWNTs completely when using a 0.8 mg.ml<sup>-1</sup> concentrated solution. Moreover, the absence of peak corresponding to Pt confirms that this catalyst might be completely embedded in a thick continuous layer of PDA. In order to determine the amount of platinum in those three systems, TGA measurements (not shown here) have been performed and lead to a platinum percentage composition estimation (wt. %) of 18%, 16% and 12% for S<sub>1</sub>, S<sub>2</sub> and S<sub>3</sub>, respectively, as expected according to the precursors compositions and concentrations.

The SEM images of MEAs show the cross-section of the edge of each sample. Firstly we can observe a porous structure for all systems, and secondly the thicknesses average is measured around 8.6 μm for S<sub>1</sub> (Fig2.A) 30 μm for S<sub>2</sub> (Fig. 2B) and 67 μm for S<sub>3</sub> (Fig2.D).

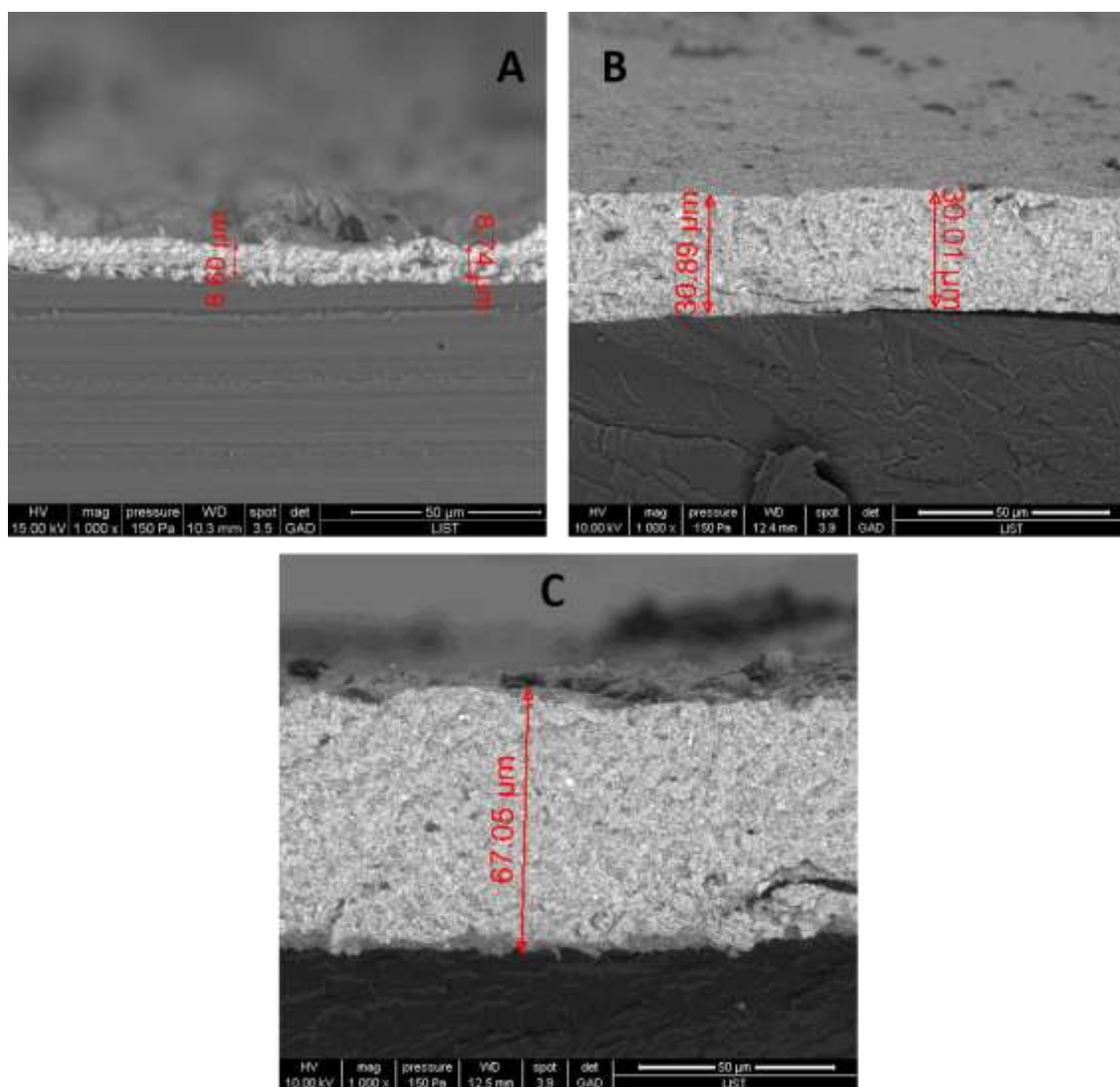
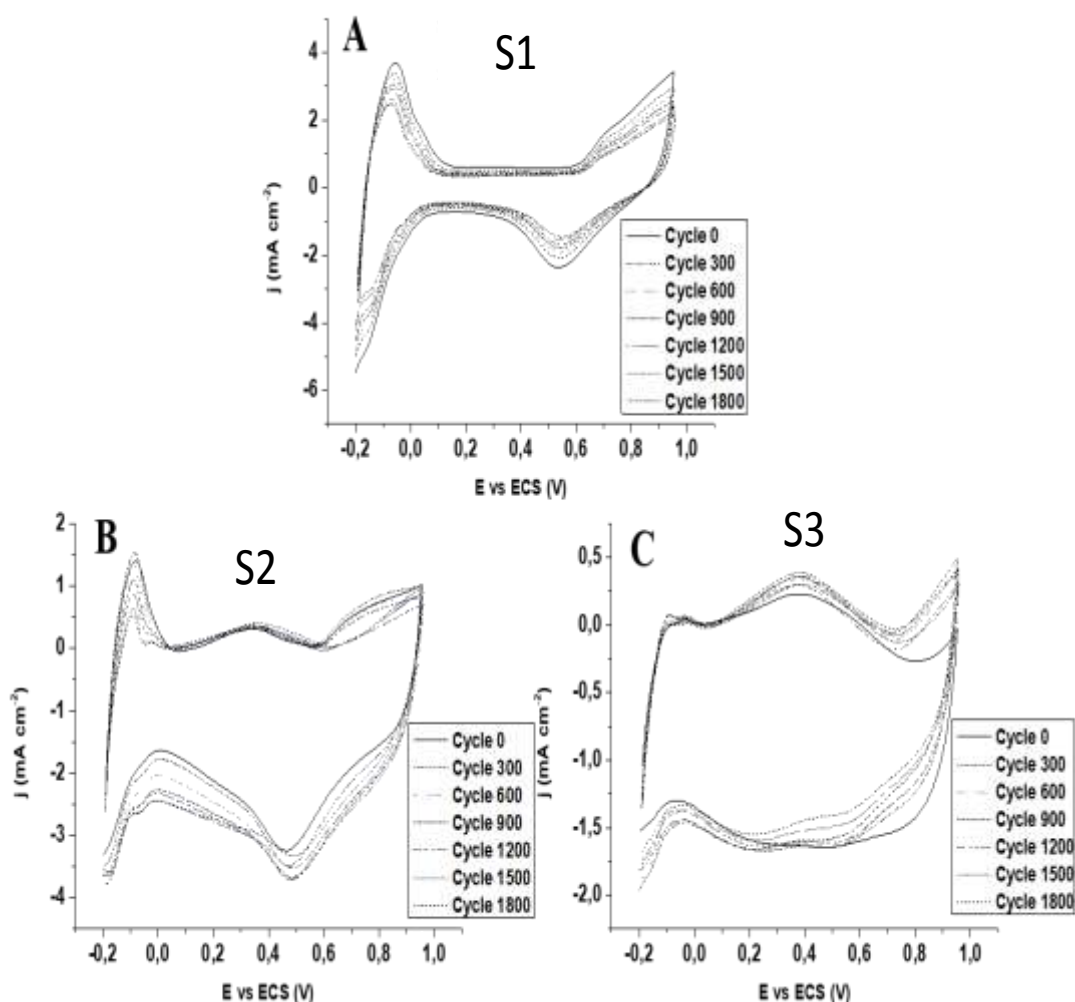


Fig. 2. SEM micrograph cross-section of catalyst layer Pt/MWNTs-PDA made with different concentration of dopamine hydrochloride: 0.2 mg.ml<sup>-1</sup> (A, corresponding to S<sub>1</sub>), 0.5 mg.ml<sup>-1</sup> (B, corresponding to S<sub>2</sub>), and 0.8 mg.ml<sup>-1</sup> (C, corresponding to S<sub>3</sub>), respectively.

The important increase of the thickness between S1 and S3 is only attributed to the higher concentration of PDA, as the volume dispersed is equal for all three systems: 200 ml. As we mentioned above, the limitations of the diffusion of reactants cause the concentration loss. The biggest thickness may not necessarily be a good factor to circumvent this problem. Cyclic Voltammetry (CV) experiments were performed with cyclic voltammetry to investigate the electrochemical behaviour of Pt/MWNTs-PDA made with different concentrations of dopamine hydrochloride.



**Fig. 3.** Voltammograms cycles (1800 cycles) of S1(A), S2 (B) and S3 (C). Data were recorded in 0.5 M  $\text{H}_2\text{SO}_4$  at 25 °C and a sweep rate of 50  $\text{mV} \cdot \text{s}^{-1}$ .

The similar behaviour in terms of oxygen adsorption/desorption ( $\text{O}_{\text{ad/des}}$ ) and hydrogen adsorption/desorption ( $\text{H}_{\text{ad/des}}$ ) can be observed in Fig. 3A and B. However, these similarities tend to change once we increase the surface coverage of the Pt/MWNTs with PDA. The Electrochemical Active Surface Area (ECSA) of Pt can be estimated using the following equation:

$$\text{ECSA} = \frac{H_{\text{ads}}}{210 \mu\text{C} \cdot \text{cm}^{-2} \cdot \text{Pt}_{\text{loading}}} \quad (3)$$

$H_{\text{ads}}$  can be obtained by integrating the average peak area after continued cycling. The Pt loading can be calculated thanks to the TGA results. The ECSA of S<sub>1</sub> and S<sub>2</sub> (Fig. 3B and C) are 5.2  $\text{m}^2 \cdot \text{g}_{(\text{Pt})}^{-1}$  and less than 0.2  $\text{m}^2 \cdot \text{g}_{(\text{Pt})}^{-1}$ , respectively. The ECSA tends to decrease in terms of  $H_{\text{ad/des}}$  and  $\text{O}_{\text{ad/des}}$  when we increase the surface coverage of MWNTs with PDA, meaning that the excess of PDA might affect the 3D structure of MEA.

Moreover, additional peaks appear at  $E \sim 0.3$  V for both S<sub>2</sub> and S<sub>3</sub>. This could correspond to the quinone (Q) and hydroquinone (HQ) redox reactions coming from polydopamine formation. The high intensity of this peak along with the disappearance of the peaks corresponding to oxygen adsorption/desorption ( $\text{O}_{\text{ad/des}}$ ) and hydrogen adsorption/desorption ( $\text{H}_{\text{ad/des}}$ ) strongly highlight the fact that Pt nanoparticles are not available for catalytic reaction because fully embedded in PDA. Nevertheless, no inclination of the different voltammograms cycles is observed, meaning that the conductivity of PDA-MWNTs stays stable during the measurement.

After CV tests of Pt/MWNTs-PDA, polarization curves were collected by optimizing the parameters for each MEA via single cell measurements. Power densities of 350 mW.cm<sup>-2</sup> and 600 mW.cm<sup>-2</sup> (Fig.4) were reached for the S<sub>1</sub> and S<sub>2</sub>, respectively, which is higher than the measured standard Pt/CB (Carbon Black) electrodes with Pt loading of 0.02mg.cm<sup>-2</sup>. With the S<sub>3</sub> sample, no recordable polarization curve could have been recorder, due to its high resistivity.

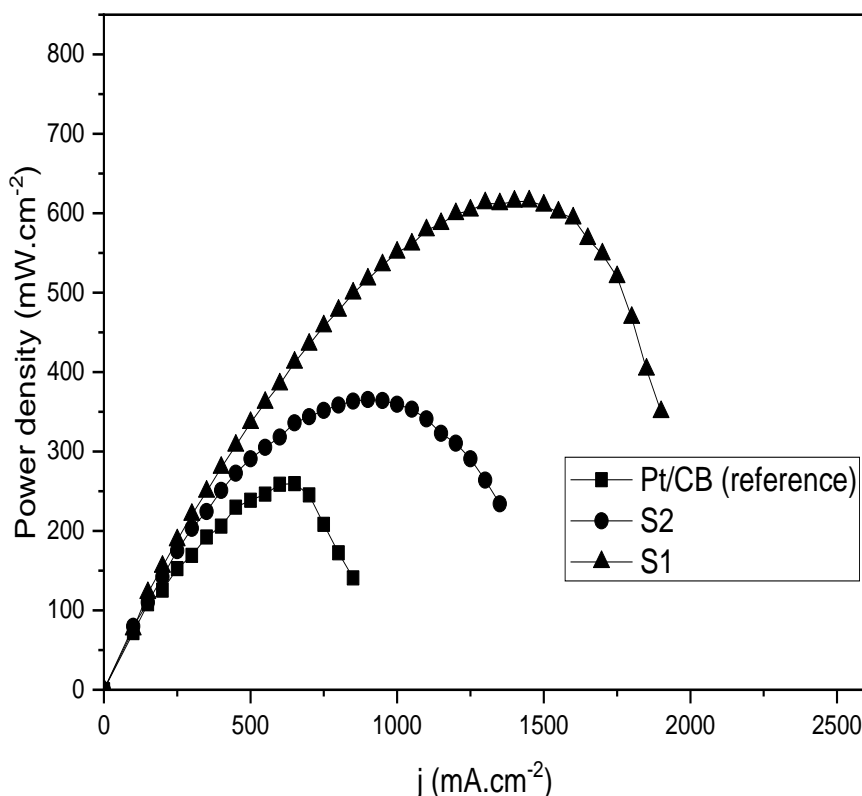


**Fig. 4.** Power density curves of fuel cell Pt/CB (used as the reference), and (Pt/MWNTs-PDA) made with different concentrations of dopamine hydrochloride: (S<sub>1</sub>) 0.2 mg.ml<sup>-1</sup> and (S<sub>2</sub>) 0.5 mg.ml<sup>-1</sup>, respectively.

Regarding to the polarization curve we can easily assume that the excess of PDA seems to drastically affect the conductivity inside the electrode membrane. Moreover, this can be explained by a loss of the electrical conductivity when the concentration of PDA is increased. Electrical conductivities measured by “four point probes” clearly show the conductivity decrease from 1.628x10<sup>0</sup> to 1.318x10<sup>-2</sup> (Table 2) when the surface coverage of PDA increases.

| Sample         | Conductivity (S.cm <sup>-1</sup> ) |
|----------------|------------------------------------|
| S <sub>1</sub> | 1.628x10 <sup>0</sup>              |
| S <sub>2</sub> | 1.950x10 <sup>-1</sup>             |
| S <sub>3</sub> | 1.318x10 <sup>-2</sup>             |

**Table 2:** Electrical conductivities of Pt/MWNTs-PDA made with different concentration of dopamine hydrochloride: 0.2 mg ml<sup>-1</sup> (corresponding to S<sub>1</sub>), 0.5 mg.ml<sup>-1</sup> (corresponding to S<sub>2</sub>), and 0.8 mg.ml<sup>-1</sup> (corresponding to S<sub>3</sub>), respectively.

Here the carbon nanotubes are segregated from one another which decrease the electrical conductivity. Furthermore, the diffusion of reactants to the catalyst at high current densities (starts at 1400 mA.cm<sup>-2</sup> and 1800 mA.cm<sup>-2</sup>) can contribute to the concentration loss as well. This might be the reason why the thickness plays such an important role in fuel cell environment.

The difference in terms of concentration polarization may be due to the incapability of the catalyst support system to maintain the initial concentration of the reactants, which causes a gradient of concentration.

#### IV. CONCLUSION

This paper demonstrated an optimization approach allowing us to understand how the coverage of Pt/MWNTs with PDA influence the performance of MEAs. It is clear that PDA is a very promising candidate for PEMFC as it is the case for 51,2% and 88,2% of the surface coverage of PDA. We highlight here the fact that the PDA plays an important role in electrodes, allowing to significantly improve the performance of fuel cells compared to commercial Carbon black (Pt/CB) without PDA (used as standard reference). However, when the coverage rate is too high (above 90%), the performance is dramatically reduced. Conductivity measurements have shown that high PDA concentration tends to affect the electrical conductivity, leading to a drop in power densities.

Moreover, the structure of electrodes tends to get thicker and more compact when the concentration of PDA is increased, leading to low catalytic accessibility and which might be the reason why the performance of MEAs decreased.

#### ACKNOWLEDGEMENTS

Financial support of the Fond National de la Recherche Luxembourg (FNR-CORE «EnergyCell» C13/MS/5897111, duration 36 Months).

#### REFERENCES

- [1]. J. Larminie, A. Dicks, Fuel Cell Systems Explained, first ed., John Wiley & Sons Ltd, UK, **2001**.
- [2]. R. O'Hayre, S. Cha, W. Colella, F. B. Prinz, Fuel Cell Fundamentals, John Wiley & Sons, New York, USA **2009**.
- [3]. Y. Shao, G. Yin, Z. Wang, Y. Gao, J. Power Source. **2007**, 167, 235-242.
- [4]. S. Sharma, B. G. Pollet, J. Power Source. **2012**, 209, 96-119.
- [5]. S. Srinivasan, O. A. Velev, A. Parthasarathy, D. J. Manko, A.J. Appleby, J. Power Sources. **1991**, 36, 299-320.
- [6]. S. Srinivasan, E. A. Ticianelli, C. R. Derouin, A. Redondo, J. Power Sources. **1988**, 22, 359-375.
- [7]. B. Lim, M. Jiang, P. H. C. Camargo, E. C. Cho, J. Tao, X. Lu, Y. Zhu, Y. Xia, Science. **2009**, 324, 1302-1305.
- [8]. K. D. Beard, D. Borrelli, A. M. Cramer, D. Blom, J. W. Van Zee, J. R. Monnier, ACS Nano. **2009**, 3, 2841-2853.
- [9]. Y. Choi, D. Higgins, Z. W. Chen, J. Electrochem. Soc. **2012**, 159, B87-B90.
- [10]. R. O'Hayre, D.R. Barnett, F.F. Prinz, J. Electrochem. Soc. **2005**, 152, A439-A444.
- [11]. R. O'Hayre, S. J. Lee, S.W. Cha, F. B. Prinz, J. Power Sources. **2002**, 109, 483-493.
- [12]. A. D. Taylor, B. D. Lucas, L. J. Guo, L. T. Thompson, J. Power Sources. **2007**, 171, 218-223.
- [13]. M. S. Wilson, S. Gottesfeld, J. Applied electrochemistry. **1992**, 22, 1-7.
- [14]. M. Michel, A. Taylor, R. Sekol, P. Podsiadlo, P. Ho, N. Kotov, L. Thompson, Adv. Mater. **2007**, 19, 3859-3864.
- [15]. G. Decher, Science. **1997**, 277, 1232-1237.
- [16]. M. Michel, F. Ettingshausen, F. Scheiba, A. Wolz, C. Roth, Phys. Chem. Chem. Phys. **2008**, 10, 3796-3801.
- [17]. A.D. Taylor, M. Michel, R.C. Sekol, J.M. Kizuka, N.A. Kotov, L.T. Thompson, Adv. Funct. Mater. **2008**, 18, 3003-3009.
- [18]. A. Wolz, S. Zils, M. Michel, C. Roth, J. Power Sources. **2010**, 195, 8162-8167.
- [19]. H. Long, D. Del Frari, A. Martin, J. Didierjean, V. Ball, M. Michel, H. Ibn El Ahrach, J. Power Sources. **2016**, 307, 569-577.
- [20]. A. Wolz, S. Zils, D. Ruch, N. Kotov, C. Roth, M. Michel, Adv. Energy Mater. **2012**, 2, 569-574.
- [21]. J.E. Endoh, S. Terazono, H. Widjaja, Y. Takimoto. Electrochemical and solid-state letters. **2004**, 7, A209-A211.
- [22]. F. de Bruijn, V. Dam, G. Janssen, Fuel cells. **2008**, 8, 3-22.
- [23]. L. M. Roen, C. H. Paik, T. D. Jarvi, Electrochemical and solid-state letters. **2004**, 7, A19-A22.
- [24]. V. Ball, D. Del Frari, M. Michel, M. J. Buehler, V. Toniazzo, M. K. Singh, J. Gracio, D. Ruch, BioNanoSci. **2012**, 2, 16-34.

Hongtao Long, et.al "Multilayered Carbon nanotubes/polydopamine-based electrodes for hydrogen fuel cells: effect of polydopamine coverage rates on power densities" *International Journal of Research in Engineering and Science (IJRES)*, vol. 08(1), 2020, pp. 48-55.